Possible nodal vortex state in $CeRu_2$

R. Kadono, W. Higemoto, and A. Koda
Institute of Materials Structure Science, High Energy Accelerator Research Organization (KEK), Tsukuba, Ibaraki 305-0801, Japan

K. Ohishi, T. Yokoo,* and J. Akimitsu*
Department of Physics, Aoyama-Gakuin University, Setagaya, Tokyo 157-8572, Japan

M. Hedo,† Y. Inada, and Y. Ōnuki‡
Graduate School of Science, Osaka University, Toyonaka, Osaka 560-0043, Japan

E. Yamamoto and Y. Haga
Advanced Science Research Center, Japan Atomic Energy Research Institute, Tokai, Ibaraki 319-1195, Japan
(Received 15 December 2000; published 24 May 2001)

The microscopic property of magnetic vortices in the mixed state of a high-quality $CeRu_2$ crystal has been studied by muon spin rotation. We have found that the spatial distribution of magnetic induction $\mathbf{B}(\mathbf{r})$ probed by muons is perfectly described by the London model for the triangular vortex lattice with appropriate modifications to incorporate the high-field cutoff around the vortex core and the effect of long-range defects in the vortex lattice structure at lower fields. The vortex core radius is proportional to $H^{(\beta-1)/2}$ with $\beta \simeq 0.53$ (H being the magnetic field), which is in good agreement with the recently observed nonlinear field dependence of the electronic specific heat coefficient $\gamma \propto H^{\beta}$. In particular, the anomalous increase of magnetic penetration depth in accordance with the peak effect in dc magnetization ($\geqslant H^* \simeq 3$ T at 2.0 K) has been confirmed; this cannot be explained by the conventional pair-breaking effect due to magnetic field. In addition, the spontaneous enhancement of flux pinning, which is also associated with the peak effect, has been demonstrated microscopically. These results strongly suggest the onset of collective pinning induced by a new vortex state having an anomalously enhanced quasiparticle density of states for $H \geqslant H^*$.

DOI: 10.1103/PhysRevB.63.224520 PACS number(s): 74.60.−w, 74.25.Ha, 74.70.Ad, 76.75.+i

I. INTRODUCTION

Since its discovery in the late 1950s by Matthias *et al.*,[1] superconductivity in $CeRu_2$ with the $C15$ cubic Laves phase structure has been drawing continuing interest. Studies in the early stage were mostly focused on the coexistence of magnetism and superconductivity because of the unusual insensitivity of the superconductivity to alloying with magnetic elements.[2–5] The primary aspect of the recent interest lies in the nature of $4f$ electrons that yields the possibility of studying the role of electronic correlation in superconductivity, on which much progress has been made in recent years. Contrary to the earlier speculation that Ce ions are tetravalent with all $4f$ electrons contributing to s, p, and d bands, studies using various spectroscopic techniques, including photoemission,[6–12] x-ray absorption,[13] and inelastic neutron scattering,[14] have provided strong evidence that $CeRu_2$ is a mixed valent compound with nearly $4f^1$ occupation. On the other hand, there is mounting experimental evidence that the $4f$ electrons are itinerant, as typically demonstrated by the de Haas–van Alphen measurement.[15,16] Recent band-structure calculations have shown that the $4f$ electrons form a strongly hybridized band with conduction electrons with the average $4f$ electron count being close to unity.[17–19] The relatively small enhancement of the cyclotron mass ($\simeq 0.6-8 m_0$, which is about three times the calculated band-electron mass[16]) as well as the electronic-specific-heat coefficient γ [$\simeq 30$ (mJ/mol)/K^2, which suggests an approximately 2.5-times enhanced density of states at the Fermi surface[20,21]] support the quasi-one-electron picture, although there seems to remain a residual influence of on-site Coulomb interaction.

Thus, the revelation of relatively weak electronic correlation in $CeRu_2$ leads us to the expectation that the superconductivity in this compound would be of conventional BCS type, as suggested by the highest transition temperature ($T_c \simeq 6.1-6.5$ K) among Ce intermetallic compounds. However, recent studies have shown some distinct features that compel careful reexamination of such a naive presumption. While the pairing symmetry was determined to be s wave by various measurements including those of specific heat,[20] nuclear quadrupole resonance (NQR),[22,23] and microwave response,[24] a detailed study of spin-lattice relaxation in NQR suggests an anisotropic energy gap.[25] The nonlinear field dependence of γ in the mixed state suggests a close link with such an anisotropic order parameter, in addition to the field-induced anisotropic pair breaking effect.[21] This is also related to the surprising result that the de Haas–van Alphen oscillation can be observed deep in the mixed state of $CeRu_2$ where the cyclotron radius is much larger than the intervortex distance.[16] Moreover, the presence of weak magnetism coexisting with superconductivity is strongly suggested,[26,27] which may play some implicit role in the related issues.

Meanwhile, the origin of large hysteresis in the isothermal dc magnetization near the upper critical field H_{c2} (or so-called ''peak effect'') has been an issue of considerable attention because of the possibility of an associated novel mixed state. The related anomaly was first observed as an

enhanced paramagnetic magnetization,[28] which was followed by the observation of irreversible magnetization.[20,29] Although the peak effect is rather commonly observed in clean type-II superconductors and is usually explained by the increase of net pinning force due to the softening of the flux line lattice (FLL) and associated optimization of the vortex configuration along with randomly distributed pinning centers,[30–32] the one observed in $CeRu_2$ turned out to exhibit an additional feature of field and temperature hysteresis at the onset of the irreversible region.[26,33–36] This hysteresis has been interpreted as a manifestation of the first-order phase transition to a further inhomogeneous novel mixed state predicted by Fulde-Ferrel-Larkin-Ovchinnikov (FFLO).[37,38] The FFLO state has been predicted to occur in clean type-II superconductors (i.e., electronic mean free path l is much longer than the superconducting coherence length ξ_0) with large Pauli paramagnetic spin susceptibility χ_s of the conduction electrons and a large Ginzburg-Landau parameter κ.[39] The system satisfying the latter two conditions can reach the Clogston-Chandrasekhar (CC) limit where the spin polarization (Zeeman) energy $\chi_s H^2/2$ is comparable with the superconducting condensation energy $H_c^2/8\pi$ at fields H near H_{c2}. The recent model including the effect of orbital current predicts that the system near the CC limit falls into a new inhomogeneous state (generalized FFLO state or GFFLO state) at a field H_i below H_{c2} where the order parameter is spatially modulated with periodic planar nodes aligned perpendicular to the vortices.[40] It also predicts that the transition is of the first-order at both H_i and H_{c2}. The possibility of the FFLO state was first pointed out in a heavy-Fermion superconductor UPd_2Al_3 based on magnetostriction measurements,[41] followed by other candidates including UPt_3 (Ref. 42) and UBe_{13}.[43]

Unfortunately, further experimental investigations to confirm the presence of the FFLO (or GFFLO) state in $CeRu_2$ are largely divided in their conclusions. Detailed studies of the magnetization process have led to both affirmative[44–53] and negative[54–59] arguments, indicating the difficulty of interpreting these data unambiguously. The most critical arguments based on the magnetization and transport[60–63] measurements may be summarized in the following points.

(1) The peak effect is rather insensitive to impurities and is observed in the specimen that is not in the clean limit,[55,56,63] whereas the FFLO state is predicted to occur for those in the clean limit. In particular, the pinning force does not decrease with increasing spin susceptibility, as indicated by the effect of La doping.[56]

(2) The enhanced pinning is observed in the temperature region near T_c,[60,61,63] whereas most theories on the FFLO state predict that it exists only below the critical point $T^* = 0.55 - 0.56 T_c$.[39,64]

(3) The Maki parameter κ_2 increases with decreasing temperature,[21,59] whereas it is expected to behave oppositely when the system is near the CC limit.[65]

(4) There is no clear indication of the first-order phase transition in the most recent magnetization measurements on the best-quality specimen using a Faraday force magnetometer.[59]

We note that there are many other less critical arguments that the observed phenomena are explained essentially within the conventional pinning mechanism. However, we should recognize that these points must be carefully scrutinized on the basis of the following counterarguments.

(1) It should be remembered that the mechanism of spontaneous increase of the pinning force between the conventional and the FFLO case has no essential difference in the sense that it is due to the softening of FLL. Both the conventional softening and that due to the occurrence of the FFLO state can coexist, making it difficult to distinguish one from the other. Thus, the first two points might be explained by the mixed effect of these two origins. As to the effect of La doping, it should be noted that the decrease of the pinning force for the single vortex is readily compensated by the increase of the collective pinning force, which is the essence of collective pinning. Needless to say, the bulk magnetization is sensitive only to the total pinning force.

(2) It has been revealed that the magnitude of the paramagnetic moment in $CeRu_2$ measured by neutron diffraction does not decrease below T_c at 3 T,[66] while it is expected to decrease in the clean limit due to the formation of *s*-wave Cooper pairs [this is actually observed in V_3Si (Ref. 67)]. Thus, the situation in $CeRu_2$ is that the paramagnetism is not suppressed by superconductivity, suggesting an enhanced presence of quasiparticles near H_{c2}. The behavior of κ_2 should be assessed carefully in light of this anomalous paramagnetism.

In addition to these, the results in Ref. 59 typically exemplify the complexity of the magnetization measurements and their interpretation, as was also revealed by earlier works. It is clear that microscopic information is definitely needed to unravel this complicated issue in terms of the mechanism of FLL softening. This work is devoted to the search for microscopic clues to distinguish the origin of FLL softening in $CeRu_2$.

The muon spin rotation (μSR) technique provides a powerful tool for obtaining microscopic information of FLL in the type-II superconductors. Implanted muons randomly probe the local magnetic field produced by the FLL, yielding the field distribution profile from which one can directly derive magnetic penetration depth λ and vortex core radius ρ_v. In the first attempt to obtain such information for $CeRu_2$ by the μSR technique, we found an anomalous increase of the penetration depth in the magnetic field region where the peak effect was observed.[68] The enhanced λ effectively corresponds to the enhanced normal state carrier density; this is consistent with the emergence of the GFFLO state.

In this paper, we report on our new μSR measurements of the mixed state of $CeRu_2$ with much improved single crystals. Following a brief description on the experiment and data analysis, we will present the superconducting parameters (λ, ρ_v, etc.) versus magnetic field and temperature determined by μSR. Then, the response of FLL to the variation of the external magnetic field as observed by μSR will be presented to provide microscopic basis for the interpretation of bulk magnetization measurements. Lastly, after a critical review of earlier arguments concerning the FFLO state, the nature of the mixed state in $CeRu_2$ near H_{c2} will be discussed in light of the present μSR results.

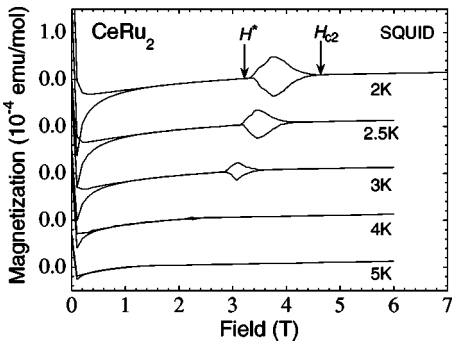

FIG. 1. Isothermal dc magnetization of the single-crystalline $CeRu_2$ specimen with rrr≃91, where the field was parallel to [100].

II. EXPERIMENTAL DETAILS

Single crystals of $CeRu_2$ were grown by the Czochralski pulling method from a solution of 4N (99.99% pure) Ce and 4N Ru in a tetra-arc furnace. The crystals were purified by solid-state electrotransport annealing at 700–800 °C under a high vacuum of 10^{-10} Torr. The ingots were determined to be single crystals from x-ray Laue patterns. The residual resistivity ratio [rrr$\equiv\rho_{RT}/\rho_0$, i.e., the resistivity at ambient temperature ρ_{RT} divided by the residual resistivity ρ_0 at low temperatures (RT is room temperature)] was 91, which is to be compared with rrr≃30 of the previous specimen.[68] The crystals were further characterized by magnetization measurement using a superconducting quantum interference device (SQUID) magnetometer to identify the region of the peak effect. The field-dependent magnetization and corresponding H-T phase diagram for the present specimen are shown in Figs. 1 and 2.

The μSR measurements were performed on the M15 beam line at TRIUMF that provides a beam of nearly 100% spin-polarized positive muons of momentum 28.6 MeV/c. A μSR spectrometer ''Belle'' with high time resolution was used to measure the decay positron time spectra under a transverse field of up to 4 T. A schematic configuration around the central part of the spectrometer is shown in Fig. 3. The specimen was field-cooled at measured magnetic fields to determine the field dependence of the superconducting parameters. The details of the procedure for the measurements with varying external field will be described later (see Sec. IV B). Muons were implanted into the specimen (measuring about 7 mm×7 mm and 0.5 mm thick) after passing through a 3-mm-diameter collimator. The initial muon spin polarization was perpendicular to the magnetic field H (and the c axis where $H\|c$) and thus to the FLL in the superconducting state.

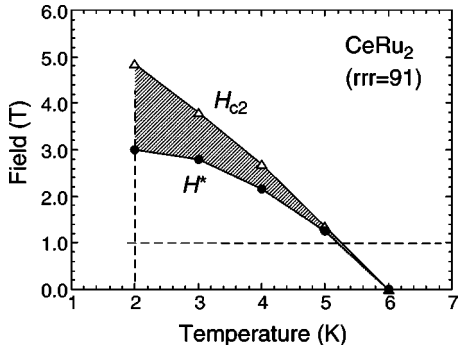

FIG. 2. H-T phase diagram of $CeRu_2$, where the peak effect region defined by H^* and H_{c2} in Fig. 1 is shown as the hatched area.

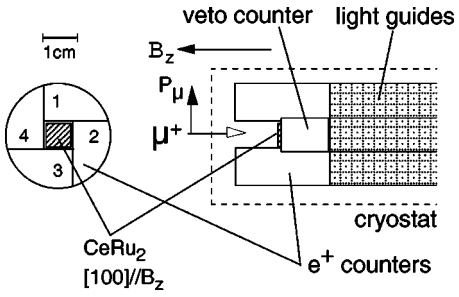

FIG. 3. A schematic view of the Belle spectrometer. Muons are implanted from the left with the initial polarization P_μ perpendicular to the external field H_z. The signal from the muons that missed the specimen is discriminated by the veto counter.

III. DATA ANALYSIS

Since the muons stop randomly on the length scale of FLL, the muon spin precession signal provides a random sampling of the internal field distribution in the mixed state. In this case, the real amplitude of the Fourier-transformed time spectrum corresponds to the internal field distribution $n(B)$, i.e.,

$$n(B)=\mathrm{Re}\left[\gamma_\mu\int[P_x(t)+iP_y(t)]\exp(i\gamma_\mu Bt)dt\right], \tag{3.1}$$

where $\gamma_\mu=2\pi\times135.54$ MHz/T, B is the magnetic induction, and

$$P_x(t)=\frac{1}{A_0}\left[\frac{N_1(t)-N_3(t)}{N_1(t)+N_3(t)}\right], \tag{3.2}$$

$$P_y(t)=\frac{1}{A_0}\left[\frac{N_2(t)-N_4(t)}{N_2(t)+N_4(t)}\right], \tag{3.3}$$

are the complex muon polarization with $N_j(t)$ $(j=1,2,3,4)$ being the time-differential positron counts of the four counters shown in Fig. 3 and A_0 the initial decay positron asymmetry (after corrections for background and instrumental asymmetry). Figure 4 shows typical examples of the frequency spectra [$=A_0n(B)$] at 2 K deduced by fast Fourier transformation (FFT). An appropriate apodization was performed to reduce the satellite structure in the FFT spectrum due to the finite time window (=3.2 μs), so that the relative height of the satellite peaks should be less than 0.02.[69] Since it is not clear how the statistical errors in the time spectra propagate upon FFT, the errors in the FFT spectra were estimated from the fluctuation of the FFT signals outside the peak region. H_{c2} is about 5 T at this temperature and thus all the spectra in Fig. 4 reflect the field distribution of the mixed

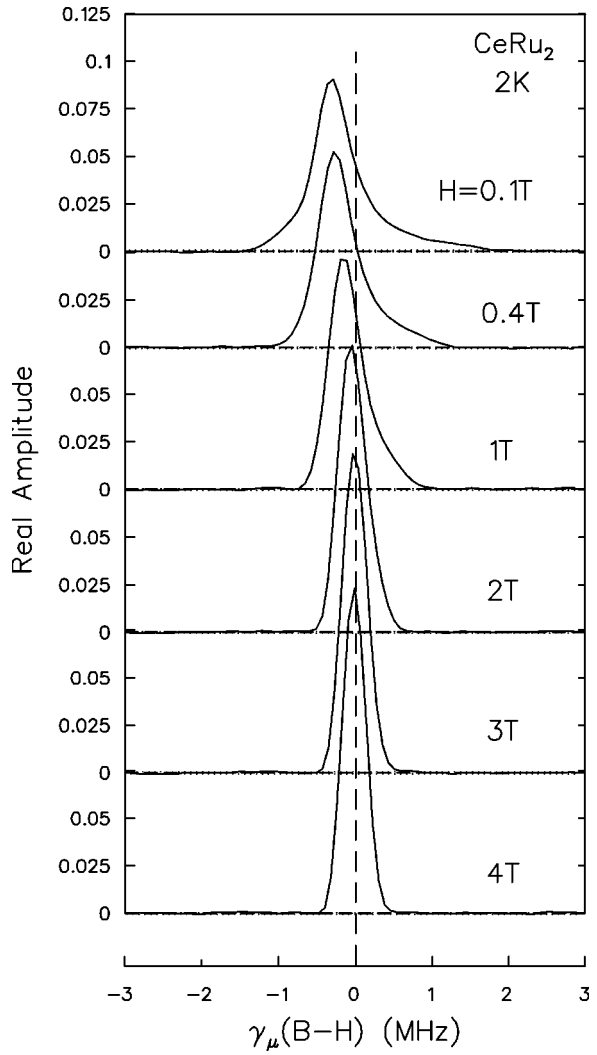

FIG. 4. The Fourier transform of the μSR signals observed in $CeRu_2$ at 2 K, where the real amplitude corresponding to the magnetic field distribution is plotted.

state for each field. The probability that muons probe the field at saddle points is maximum where the field is lower than the applied external field H. Since the average field $\int Bn(B)dB$ is close to H, the function $n(B)$ has an asymmetric distribution with respect to H. In Fig. 4 the FFT spectra are plotted against $B-H$ so that this asymmetry can be clearly seen.

In order to reconstruct a two-dimensional field distribution profile from the one-dimensional spectral density measured by μSR, one needs a model of the vortex structure. We calculated the spectral density function $n(B)$ from the field profile $B(r)$ given by the London model with a perfect triangular FLL:[70,71]

$$n(B)=\frac{dr}{dB(r)}, \tag{3.4}$$

$$B(r)=\overline{B}_0\sum_{\mathbf{K}}\frac{e^{-i\mathbf{K}\cdot\mathbf{r}}e^{-K^2\xi_v^2}}{1+K^2\lambda^2}, \tag{3.5}$$

where $\mathbf{K}$ is a translation of the vortex reciprocal lattice,

$$\mathbf{K}=l\hat{\mathbf{u}}'+m\hat{\mathbf{v}}', \quad (l,m=0,\pm1,\pm2\ldots) \tag{3.6}$$

$$\hat{\mathbf{u}}'=\frac{2\pi}{a}\frac{2}{\sqrt{3}}\hat{\mathbf{y}},$$

$$\hat{\mathbf{v}}'=\frac{2\pi}{a}\left(\hat{\mathbf{x}}-\frac{1}{\sqrt{3}}\hat{\mathbf{y}}\right), \tag{3.7}$$

with $\hat{\mathbf{x}}$ and $\hat{\mathbf{y}}$ denoting the plane of precession (normal to the vortices), B_0 ($\simeq H$) is the average internal field, λ is the penetration depth, and ξ_v is the cutoff parameter. [The lattice structure is reported to be triangular from both neutron diffraction[72,73] and scanning tunneling spectroscopy (STS) measurements.[74]] Here, it should be stressed that the cutoff parameter ξ_v cannot be simply regarded as the Ginzburg-Landau (GL) coherence length ξ or the vortex core radius, although it is indeed related to ξ. Detailed theoretical analysis indicates that ξ_v must be scaled by a factor depending on the magnetic field in order for the London model to provide a proper approximation of the GL theory.[75,76] In order to avoid a model dependence in the interpretation of the cutoff parameter, we will adopt a different definition of the vortex core radius (see below).

The theoretical line shape to be compared with μSR data in the frequency domain is then obtained by convoluting $n(B)$ with the spectrum $q(B)$ that provides a natural linewidth determined by the time window for FFT including the effect of apodization and additional broadening σ_B resulting from other sources of field inhomogeneity;

$$\overline{n}(B)=\int e^{-\sigma_B^2x^2}q(x)[(1-b_0)n(B-x)+b_0\delta(H-x)]dx, \tag{3.8}$$

where b_0 is the fractional yield of the background signals from muons stopped in the material outside the specimen. In particular, the field inhomogeneity due to the random disorder and distortion of FLL due to vortex pinning is well described by the Gaussian distribution of the fields.[70,77] The line shape $q(B)$ was determined *in situ* by measuring the μSR spectra in the normal state (which was readily attained by raising the sample temperature above T_c) and Fourier-transformed by the same procedure as at lower temperatures.

While the FFT spectra above 1 T were well reproduced by the modified London model, we found that it does not provide a satisfactory description of the total line shape for the lower field data, as shown in Figs. 5(a)–5(c). The discrepancy is characterized by the shift of the spectral weight to lower frequencies with an enhanced tail, which is not readily understood in terms of the Gaussian broadening due to random vortex pinning. Our heuristic approach has revealed that the fitting is drastically improved by introducing the fluctuation of the reciprocal vector in Eq. (3.5).

$$\mathbf{K}=l'\hat{\mathbf{u}}'+m'\hat{\mathbf{v}}', \tag{3.9}$$

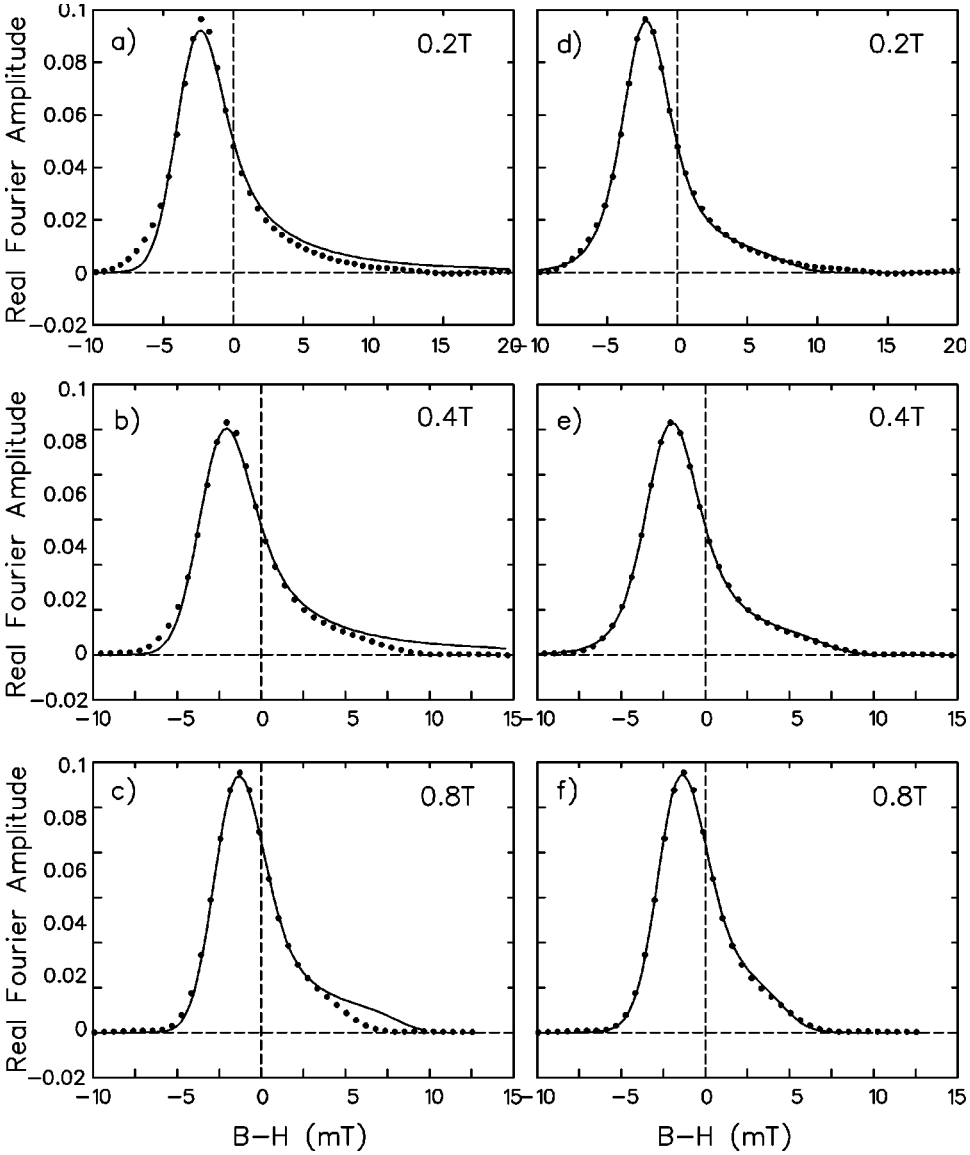

FIG. 5. The comparison of fitting results for the FFT spectra in $CeRu_2$ at 2 K. Solid curves in (a)–(c) are the best fits by Eq. (3.8), and those in (d)–(f) are ones obtained with the effect of ''random compression'' (see text).

$$l' = l(1+\delta_l), \quad m' = m(1+\delta_m) \quad (l,m = 0, \pm 1, \pm 2 \ldots) \tag{3.10}$$

$$P(\delta_k) \propto \exp(-\delta_k^2/\sigma_{lm}^2) \quad (k = l,m). \tag{3.11}$$

This fluctuation can be physically interpreted as the long-range distortion of FLL represented by the respective indices of **K** in the reciprocal space, which is illustrated in Fig. 6. As shown in Figs. 5(d)–5(f), the calculated line shape with finite values for σ_{lm} yields excellent agreement with data below 1 T. The field dependence of σ_{lm} (see the section below) strongly suggests that such a long-range distortion seems to be related with the softening of the compression modulus $C_{11}-C_{66}$ at lower magnetic fields. Thus, the effect may be called a ''random compression'' of FLL. We stress, however, that this effect is discernible only below 1 T, and has the least relevance with the main issue of the peak effect and associated anomaly at higher fields.

The alternative method of analysis is to perform it in the time domain, where the time evolution of the complex muon polarization is

$$P_x(t) + iP_y(t) = e^{-\sigma_f^2 t^2} \int_0^\infty n(B) \exp(i\gamma_\mu B t) dB, \tag{3.12}$$

where σ_f is the effective depolarization rate (corresponding to σ_B). In the present analysis, we first optimized the fitting in the frequency domain that allows direct physical interpretation, then used time-domain analysis to estimate statistical errors for the physical parameters.

IV. RESULT

A. Superconducting parameters

1. Magnetic field dependence

Before proceeding directly to the result of the fitting analysis using the modified London model, we demonstrate the anomalous field dependence of the μSR linewidth in a model-independent manner. Because of the relatively large magnetic penetration depth, the observed μSR time spectra

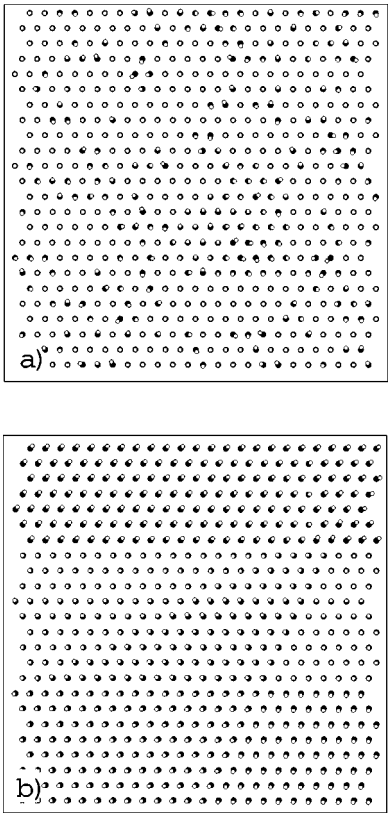

FIG. 6. (a) The effect of random vortex pinning, and (b) that of ''random compression'' leading to long-range FLL distortion, where the filled circles indicate the regular positions of vortices in the triangular lattice and open circles indicate the actual positions in the respective situations.

above $\sim$2.5 T are reasonably well reproduced by Gaussian damping with a single linewidth σ,

$$P_x(t)+iP_y(t)\simeq e^{-\sigma^2t^2}\exp(i\gamma_\mu Bt). \tag{4.1}$$

The magnetic field dependence of σ at 2 K obtained by the fitting analysis in the time domain is shown in Fig. 7. Note that the statistical errors in Fig. 7 are properly estimated from

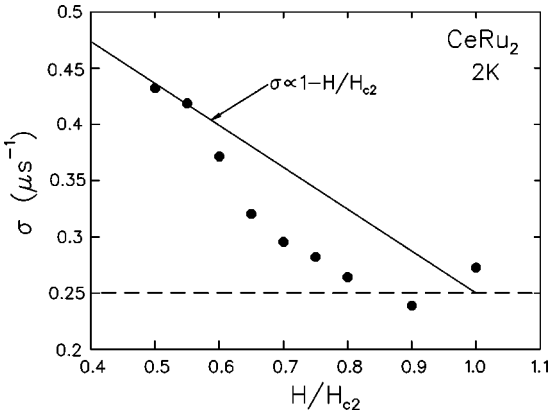

FIG. 7. Muon spin relaxation rate (linewidth) in $CeRu_2$ at 2 K deduced by analyzing the time spectra by Gaussian damping. H_{c2} is assumed to be 5 T at this temperature. Lines are guides for the eye.

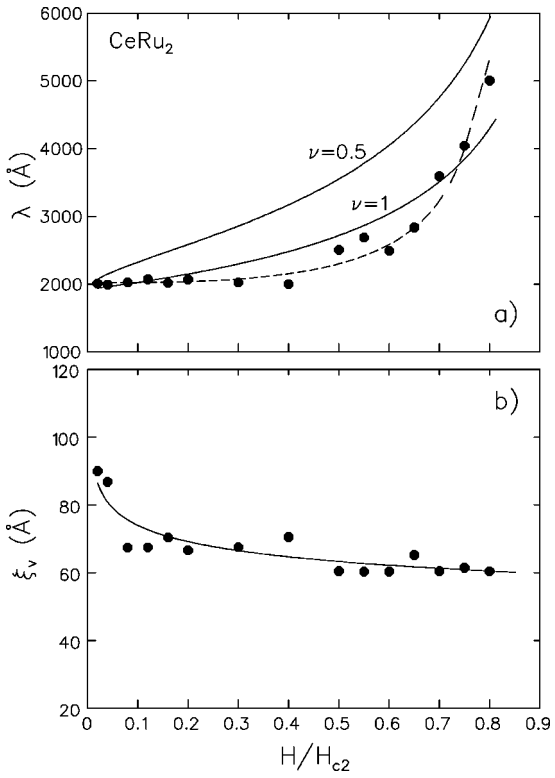

FIG. 8. (a) Magnetic penetration depth λ, and (b) high-field cutoff parameter ξ_v vs field in $CeRu_2$ at 2 K obtained by fitting data with the modified London model. Solid curves in (a) are calculated by Eq. (4.13) with $\eta=1$, while dashed line is a guide for the eye. Fitting result by Eq. (4.5) is shown in (b) as a solid curve.

the time domain analysis. The linewidth σ decreases with increasing field due to the strong overlap of vortex fields and the increasing importance of the vortex cores. According to Eq.(3.5), the field-dependent mean field variation is

$$\langle\Delta B^2\rangle\simeq 7.5\times10^{-4}(1-h)^2\phi_0^2\lambda^{-4}, \tag{4.2}$$

where $h=H/H_{c2}$ and ϕ_0 denotes the flux quantum.[70] Since the corresponding average μSR linewidth is given by

$$\sigma=\gamma_\mu(\langle\Delta B^2\rangle/2)^{1/2}\equiv\Lambda(H)\lambda^{-2}\propto 1-\frac{H}{H_{c2}}, \tag{4.3}$$

the linewidth is expected to have a linear relation with the magnetic field. However, the observed σ in Fig. 7 shows a steep decrease with increasing field for $h=H/H_{c2}>0.6$ (with presumed $H_{c2}=5$ T from Fig. 2), reaching a value almost equivalent to the natural linewidth at around $h\simeq0.8$. Note that no such singularity is expected from Eq. (3.5) considering the modest change in vortex spacing (e.g., a is 282 Å at 3 T, and 245 Å at 4 T). This result clearly demonstrates that the quasiparticle excitation is anomalously enhanced in $CeRu_2$ in this field range.

The result of fitting analysis using the modified London model indicates that this anomaly of the linewidth can be effectively attributed to that of the magnetic penetration depth λ. Figure 8 shows the field dependence of λ and the cutoff parameter ξ_v obtained from the data at 2 K. It is evi-

dent that λ is mostly independent of the field below 3 T (i.e., $h<0.6$), whereas it shows a steep increase with increasing field above 3 T. The values below 3 T ($\lambda \simeq 2000$ Å) are in good agreement with those obtained by bulk magnetization measurement.[34] On the other hand, ξ_v exhibits gradual decrease with the field (except in the lowest field range where the change is rather steep). Recent calculations for *s*-wave superconductors using quasiclassical Eilenberger equations predict the shrinkage of vortex core radius ρ_v due to vortex-vortex interaction.[78] At $T=0$ K, the calculated quasiparticle density of states (DOS) $N(H)$ is well represented by a power law H^β with $\beta=0.67$. Provided that all the DOS come from inside the vortex cores, we expect

$$N(H)=N_{\rm core}(H)\propto \pi\rho_v^2 H\propto H^\beta, \tag{4.4}$$

where the factor H is from the number of vortices per unit area, and then we have

$$\rho_v \propto H^{(\beta-1)/2}. \tag{4.5}$$

Thus, one would expect $\rho_v \propto H^{-0.165}$ at $T=0$ (i.e., $\beta=0.67$). As shown in Fig. 8, provided that $\rho_v \simeq \xi_v$ (which is only a coarse approximation, as mentioned earlier), the power law $\xi_v=\xi_0 h^{(\beta-1)/2}$ with $\beta \simeq 0.807$ and $\xi_0 \simeq 59$ Å reproduces the observed weak field dependence relatively well. However, in the following, we will define the vortex core radius more directly from the distribution of supercurrent density around the vortex core, which provides a reliable basis for comparison independent of the model used in the analysis. At this stage, we only note that the deduced ξ_v is in reasonable agreement with the coherence length ξ ($T=2$K) $\simeq 81$ Å estimated from H_{c2} ($T=2$ K), demonstrating that the parameter ξ_v introduced as a cutoff in Eq. (3.5) can be interpreted as a quantity defined by the coherence length. The large Ginzburg-Landau parameter $\kappa \simeq 30$ indicates that $CeRu_2$ is a typical type-II superconductor.

The London model gives an approximate value for λ:

$$\frac{1}{\lambda^2} \simeq \frac{4\pi n_s e^2}{m^* c^2}, \tag{4.6}$$

where m^* is the effective carrier mass and n_s is the superfluid density that may be reduced to zero toward H_{c2} as

$$n_s \propto 1-N_{\rm env}(H)/N_{\rm env}(H_{c2}), \tag{4.7}$$

where $N_{\rm env}(H)$ is the quasiparticle DOS *outside* the vortex cores. In conventional superconductors with *s*-wave pairing, the quasiparticle excitation at lower fields is mostly confined within the vortex cores. The pair-breaking excitation energy α outside the cores (which contributes to the field dependence of λ) is determined by the Zeeman energy,

$$\alpha=\mu_B H \tag{4.8}$$

in the clean limit and hence,

$$N_{\rm env}(H) \simeq \frac{\alpha}{\Delta_0}=\frac{\mu_B H}{\Delta_0}, \tag{4.9}$$

which is thus proportional to H. This leads to the linear relation

$$n_s \propto 1-\eta h, \tag{4.10}$$

where η is the parameter representing the magnitude of pair-breaking interaction and $h=H/H_{c2}$. It should be noted, however, that this relation is not valid when the field exceeds the CC limit,

$$H_p=\frac{\Delta_0}{\sqrt{2}\mu_B}, \tag{4.11}$$

or the threshold field for the FFLO state (see Sec. V). On the other hand, a nonlinear field dependence is expected for the superconductors with gapless nodes. According to Volovik, the presence of a zero-gap region on the Fermi surface (i.e., in k space) leads to a square-root dependence on H of the quasiparticle density of states.[79] This is because the density of states is predominantly determined by the contribution outside the vortex cores where the spatial motion of the quasiparticles is limited by the intervortex distance $a \sim \xi/\sqrt{h} < \lambda$. In this case, $N_{\rm env}(H)$ is scaled by $a\xi\gamma_N h \propto \sqrt{h}$ (with γ_N being the normal-state DOS) and one would expect

$$n_s \propto 1-\eta\sqrt{h} \tag{4.12}$$

with $\eta \simeq 1$ due to the predominant contribution of quasiparticle excitation outside the cores to the net DOS.

From these relations [Eqs. (4.6), (4.10), (4.12)], we derive

$$\lambda(H) \simeq \frac{\lambda(0)}{\sqrt{1-\eta h^\nu}}, \tag{4.13}$$

with $\nu=1$ (*s* wave) or 1/2 (gapless nodes). As shown in Fig. 8(a), comparison of Eq. (4.13) with the present data is far from satisfactory, particularly at higher fields where the observed λ shows a much steeper increase with increasing field. Naturally, the inclusion of enhanced quasiparticle excitation from the continuum state associated with the gapless nodes ($\nu=1/2$) does not improve the agreement. This is mainly because of the fact that such enhancement affects the field dependence of λ, especially at lower fields where $\lambda(H) \simeq \lambda(0)(1+\frac{1}{2}\eta h)$ with effectively larger η for $\nu=1/2$, while the observed anomaly is mostly in the higher-field range. Such a linear field dependence of λ has been observed by μSR in high-T_c cuprates[80] (*d*-wave pairing with line nodes) and in a class of superconductors including $2H$-$NbSe_2$ (Ref. 81) and borocarbides[82] (*s*-wave paring), where a clear tendency of greater η for larger anisotropy has been revealed. In this sense, the weak dependence on the magnetic field for $h<0.5$ is consistent with that in the case of ordinary *s*-wave pairing. In any case, the observed field dependence of λ exhibits considerable deviation from those of the conventional models.

The remaining physical parameters of our model, i.e., σ_B in Eq. (3.8) and σ_{lm} in Eq. (3.11), are related to the distortion of FLL. As mentioned earlier, σ_{lm} represents the effect of random compression, which turned out to be the predominant factor in improving the agreement between the calcu-

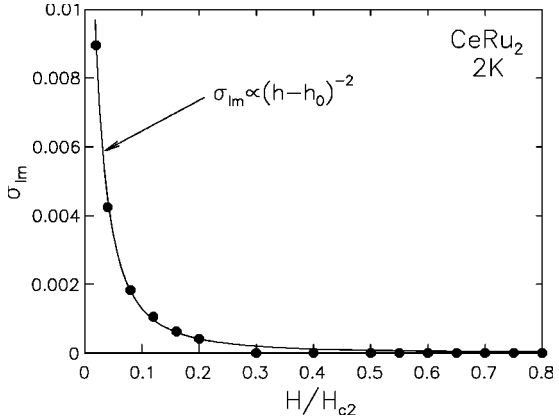

FIG. 9. The magnitude of random compression σ_{lm} vs field in $CeRu_2$ at 2 K obtained by fitting data with modulated reciprocal vectors in the modified London model. Fitting result by Eq. (4.16) is shown as a solid curve.

lated line shape and measured μSR spectra at lower fields. Compared with the effect of σ_{lm}, the values deduced for σ_B are small (0.5–1 mT below 1 T and zero for higher fields) and can thus be disregarded. Figure 9 shows the field dependence of σ_{lm} at 2 K. It exhibits a steep increase with decreasing field below $\sim$1 T, indicating that the effect is mostly associated with the low-field property of FLL. The elastic property of FLL is described by three elastic moduli: compression modulus $C_{11}-C_{66}$, shear modulus C_{66}, and tilt modulus C_{44}. The former two represent responses to the respective modes of lattice distortion within the plane perpendicular to H, whereas the last one represents the response to the tilting of vortices from the direction of H. The field dependence of these moduli over the field region far from H_{c1} is approximately expressed by

$$C_{11} \simeq C_{44} \simeq \frac{H_{c2}^2}{8\pi} h^2, \tag{4.14}$$

$$C_{66} \simeq \frac{0.13}{\kappa^2} \frac{H_{c2}}{8\pi} (1-h^2) \tag{4.15}$$

with h again being H/H_{c2}. Equation (4.14) indicates that the observed distortion is related to the softening of FLL in terms of compression and/or tilting of vortices. Provided that the vortex pinning force F_p is independent of the field (which is a reasonable assumption for low fields), we can assume Hooke's law $F_p \propto C_{ij}\sigma_{lm}$, which yields

$$\sigma_{lm} \propto \frac{F_p}{C_{ij}} \sim \frac{g}{(h-h_0)^2}, \tag{4.16}$$

for $C_{11}-C_{66}$ and C_{44}. As shown in Fig. 9, a satisfactory fit is obtained by Eq. (4.16) with $g \simeq 2.16\times10^{-5}$ and a small offset $h_0 \simeq -2.92\times10^{-2}$, indicating that σ_{lm} is related to the long-range distortion induced by random compression/tilting of vortices.

Once a satisfactory fit to the measured field distribution is obtained using the field distribution profile $n(B)$ generated

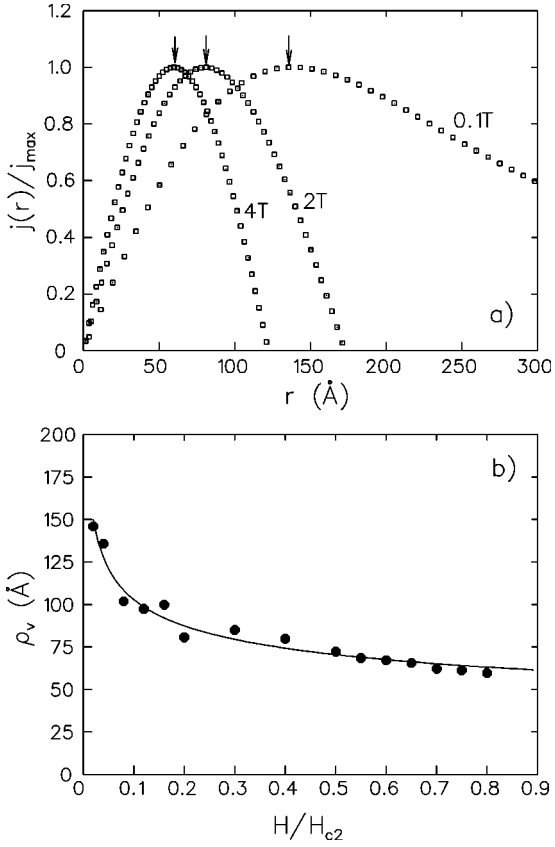

FIG. 10. (a) Supercurrent density $j(r) \propto dB(r)/dr$ in $CeRu_2$ at 2 K, calculated for $H=0.1$, 2, and 4 T from the $B(r)$ reconstructed using the modified London model. Arrows indicate the position of maximum corresponding to the effective core radius ρ_v at each field. (b) Magnetic field dependence of ρ_v, where the fitting result by Eq. (4.5) is shown as a solid curve.

from $B(r)$, one can define the vortex core radius ρ_v to be the radial distance from the vortex center at which the supercurrent density $j(\mathbf{r})$ reaches its maximum value. The supercurrent density $j(\mathbf{r})$ is obtained from the field profile $\mathbf{B}(\mathbf{r})=(0,0,B(r))$ through the Maxwell relation $j(\mathbf{r}) = |\nabla \times \mathbf{B}(\mathbf{r})|$. This feature provides an accurate and model-independent measure for monitoring the change in the effective size of vortex cores.[80,81] In Fig. 10(a), we show some examples of $j(r)$ normalized by the maximum value $j_{\max} = j(\rho_v)$, where one can clearly see that the peak of supercurrent is shifted with the field. The field dependence of ρ_v is shown in Fig. 10(b). The parameters σ_{lm} and σ_B were set to zero for the calculation of $B(r)$, to eliminate the irrelevant effect of FLL distortion. Following Eq. (4.5), a fit using the relation

$$\rho_v = \rho_0 h^{(\beta-1)/2} \tag{4.17}$$

yields satisfactory agreement with the observed dependence with $\beta=0.531$ and $\rho_0 \simeq 60$ Å . The deduced power seems to be in good agreement with that of the electronic-specific-heat coefficient $\gamma(H)$ at this temperature ($=2$ K) whereas the agreement with the model of the field-induced anisotropic gap is incomplete.[21] This result strongly suggests that the

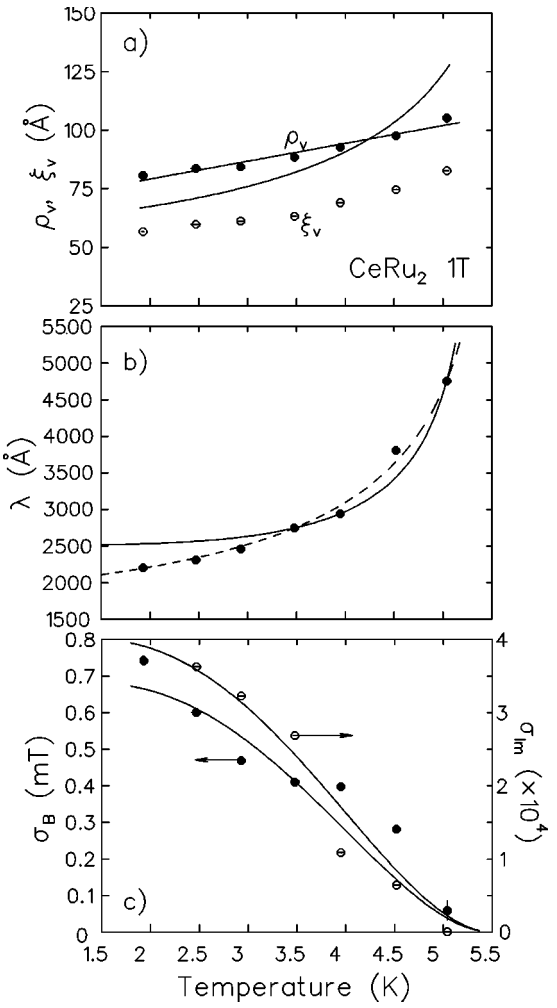

FIG. 11. Temperature dependence of the cutoff parameter ξ_v and vortex core radius ρ_v (a), the magnetic penetration depth λ (b), and those to describe the FLL distortions σ_B and σ_{lm} (c). Solid curves in (a) are fitting results by Eqs. (4.19) and (4.22), respectively, the one in (b) is a fitting result by Eq. (4.23) with $\gamma=4$, while the dashed curve is the best fit with $\gamma=1.35$, and those in (c) follow Eq. (4.27).

nearly $\sqrt{H}$ dependence of $\gamma(H)$, particularly at lower fields ($h\leqslant 0.5$) where λ behaves normally, is mainly due to that of the vortex core radius, i.e.,

$$\gamma(H)\propto N_{\rm core}(H)\propto H\pi\rho_v^2. \tag{4.18}$$

The slightly smaller value of β compared with the theoretical prediction for the *s*-wave superconductors may be explained by the anisotropy of the energy gap suggested by NQR.[25]

2. Temperature dependence

As shown earlier in Fig. 2, the temperature dependence of superconducting parameters was studied under an external field of 1 T where the peak effect is virtually absent over the entire region of temperature. Here, the primary purpose was to examine the validity of our method by measuring those parameters along a line in the *H-T* phase diagram where they are considered to behave normally. Figure 11 summarizes the results for the cutoff parameter ξ_v, penetration depth λ, vortex core radius ρ_v, long-range FLL distortion σ_{lm}, and line broadening factor σ_B for 1.9–5.0 K. The core radius ρ_v was deduced by the same procedure as used to obtain the result in Fig. 10. It is notable that the temperature dependence of ρ_v scales to that of ξ_v quite well. According to the Ginzburg-Landau theory, the temperature dependence of the coherence length near T_c is related to the upper critical field $H_{c2}(T)$ by

$$\xi(T)=\sqrt{\frac{\Phi_0}{2\pi H_{c2}(T)}}. \tag{4.19}$$

However, this is thought to be valid only along the phase boundary on the *H-T* phase diagram [i.e., $\xi(H\simeq H_{c2},T\simeq T_c)$], while little is known about the actual temperature dependence deep in the superconducting phase. It is evident in Fig. 11(a) that Eq. (4.19) with an empirical *T*-dependence for the upper critical field,

$$H_{c2}(T)=H_{c2}(0)[1-\zeta(T/T_c)^{\nu}], \tag{4.20}$$

which reproduces the data in Fig. 2 with $H_{c2}(0)=6.22$ T, $\zeta=0.876$, and $\nu=1.31$, exhibits a much steeper temperature dependence of ρ_v than that observed experimentally.

Since the work by Kramer and Pesch, who discussed the quantum effects for quasiparticles bound in the vortex cores based on the Eilenberger theory,[83,84] the actual temperature dependence of the effective core radius has been an unsettled issue to be scrutinized in more detail. The quasiparticles within the cores are subject to the Andreev reflection at the core radius and thereby form discrete bound states.[85] At lower temperatures, they occupy the lower energy levels that are confined spatially within the narrower region, leading to the shrinkage of effective core radius. They predict that the effective core radius in the clean limit superconductor would decrease linearly with decreasing temperature for $T_c^2/\varepsilon_F\ll T\ll T_c$ as

$$\xi_1(T)=\xi_{\rm BCS}\frac{T}{T_c}, \tag{4.21}$$

with $\xi_{\rm BCS}$ being the BCS coherence length and ε_F the Fermi energy. The core radius would level off at a low enough temperature where only the lowest bound state is occupied. Such an effect is suppressed in the dirty limit due to the strong damping of the quasiparticle bound states, leading to the almost constant ξ_1 over the entire temperature range. Recent theoretical calculations based on the Bogoliubov–de-Gennes approach confirmed the above prediction, where the saturation of shrinkage should occur at $T_0\simeq T_c/(k_F\xi_0)$ (with $\xi_0=v_F/\Delta_0$ and Δ_0 being the gap energy at $T=0$).[86,87] Our estimate of $k_F\xi_0\simeq 60$ for $CeRu_2$ (which would be multiplied by a factor of mass enhancement $m^*/m_0\sim 3$) indicates the saturation temperature $T_0\simeq 0.1$ K in $CeRu_2$, suggesting that the core radius would satisfy Eq. (4.21) over the current temperature range of observation. However, although our data in Fig. 11(a) indeed exhibit almost linear dependence on *T*, it is much weaker than the one predicted theoretically. The solid line in Fig. 11(a) is a fit with the relation

$$\rho_v(T)=\rho_v(0)[1+c(T/T_c)], \tag{4.22}$$

which yields the best-fit result with $\rho_v(0)=63.9$ Å and $c=0.656$. Note that one would expect $\rho_v(0)\sim 0$ when Eq. (4.21) is fully satisfied. The value of $\rho_v(0)$ is rather close to the asymptotic value ρ_0 observed at high field in the magnetic field dependence [see Eq. (4.17)]. The situation seems to be similar to the case of $NbSe_2$,[88] suggesting the presence of a common problem in the understanding of the electronic structure of vortex cores in *s*-wave superconductors.

According to the empirical two-fluid model, the temperature dependence of the magnetic penetration depth is given by

$$\lambda(T)=\frac{\lambda(0)}{\sqrt{1-(T/T_c)^{\nu}}}, \tag{4.23}$$

with $\nu=4$. As shown in Fig. 11(b), while it gives a reasonable description of the observed temperature dependence for λ with $\lambda(0)\simeq 2512$ Å , the data exhibit slight deviation from Eq. (4.23). This result is qualitatively in good accord with the one obtained from bulk measurement,[34] where a similar trend of deviation was also reported. More specifically, the observed $\lambda(T)$ shows weaker curvature than that of Eq. (4.23) with $\lambda(T\rightarrow 0)\sim 2000$ Å . This asymptotic value is close to the one estimated from specific heat[21] and from microwave response.[24] Following Ref.24, an analysis using[89]

$$\lambda(T)\simeq\frac{\lambda(0)}{\sqrt{1-(2\pi\bar{\Delta}_0/t)^{1/2}\exp(-\bar{\Delta}_0/t)}} \tag{4.24}$$

(with $\bar{\Delta}_0=\Delta_0/k_BT_c$ and $t=T/T_c$) for $0.3<t<0.6$ yields $\lambda(0)\simeq 2120$ Å and $\Delta_0\sim 3.0$. Although the value of Δ_0 points to the weak coupling limit, this should not be taken too seriously since the result is based on the analysis over a very limited temperature range (including only three data points). In any case, the observed temperature dependence for λ at $H=1$ T is understood within the conventional theory.

Finally, we show in Fig. 11(c) that the parameters representing the FLL distortion, σ_B and σ_{lm}, decrease with increasing temperature. This tendency is understood in terms of the reduction of pinning energy U at higher temperatures, i.e.,

$$\sigma_B,\sigma_{lm}\propto U(T) \tag{4.25}$$

$$U(T)=\frac{1}{8\pi}H_c^2(T)[\rho_v(T)]^n, \tag{4.26}$$

where $H_c(T)$ is the thermodynamical critical field and n takes integer values depending on the details of the pinning mechanism. The temperature dependence of $H_c(T)$ deduced from the electronic specific heat follows $H_c(0)[(1-t^2)+D(t)]$ with the deviation $D(t)$ always being smaller than 0.01 ($t=T/T_c$).[21] Using Eq. (4.22) for $\rho_v(T)$, we have

$$U(t)=U_0(1-t^2)^2(1+ct)^n, \tag{4.27}$$

which shows a monotonic decrease with decreasing temperature. Results of fitting by the above T dependence with $n=2$ are shown in Fig. 11(c) which indicates that Eq. (4.27) explains the observed trend qualitatively. The relatively strong pinning at higher temperature seen in σ_B can be understood by considering the distribution of pinning energy. The pinning centers having greater pinning potential would be more effective at higher temperatures compared with weak pinning centers, leading to the relative enhancement of distortion toward T_c. Comparison between σ_B and σ_{lm} suggests that the random pinning is more sensitive to such distributions of the pinning potential. This may be intuitively understood by considering that the long-range distortion represented by σ_{lm} is determined by the average net pinning energy over the correlated region.

B. Magnetic response of flux line lattice

Vortex pinning is one of the most complicated issues in the physics of the mixed state. This is mainly because the real nature of pinning centers is largely unknown and uncontrolled under conventional experimental conditions. This situation often leads to a sample dependence of each measurement, making it difficult to ensure reproducibility among different samples. In particular, the results of magnetization measurements in $CeRu_2$ between those by conventional SQUID and Faraday methods[59] suggest that there may be problems in clarifying the microscopic nature of vortex pinning relying solely on the bulk magnetization. Here,we demonstrate that the distortion of FLL indeed depends on the step size of field change and therefore on the details of the actual magnetization process.

Figure 12 shows the comparison of the FFT spectra between those obtained after cooling the specimen to 2 K under an external field (''field cooling'' or FC) and others obtained after cooling to 2 K under zero field (''zero field cooling'' or ZFC) followed by application of the field. The ramping rate of the external field was about 0.2 T/min. Note that the frequency range of Fig. 12(b) (=20 MHz) is much larger than that of Fig. 12(a) (=5 MHz). It is obvious that the spectra at 2 T exhibit little difference between FC and ZFC conditions, except a small downshift of central field for ZFC data (which may be an instrumental artifact), while at 4 T, the spectrum under ZFC shows a much broader line shape than that under FC. Thus, these data indicate that the FLL distortion is negligible when the external field is changed in large steps to 2 $T<H^*$, but it becomes extremely large when the field is ramped above H^*. These results are perfectly in line with the interpretation based on the SQUID magnetization measurements (e.g., Fig. 1) that the vortex pinning is weak below H^* and spontaneously becomes strong above H^*.

However, the situation is different when the external field is changed in small steps. In Fig. 13, the spectra obtained at respective fields under the FC condition are shown in comparison with those after isothermally changing the field by 0.01 T. This change would lead to the downshift of the central frequency by 1.355 MHz when the FLL is rearranged accordingly. The general tendency is again consistent with the interpretation deduced from Fig. 12, i.e., the spectrum at 2.5 T seems to follow the change in the external field while about half of the spectral weight remains at the previous field

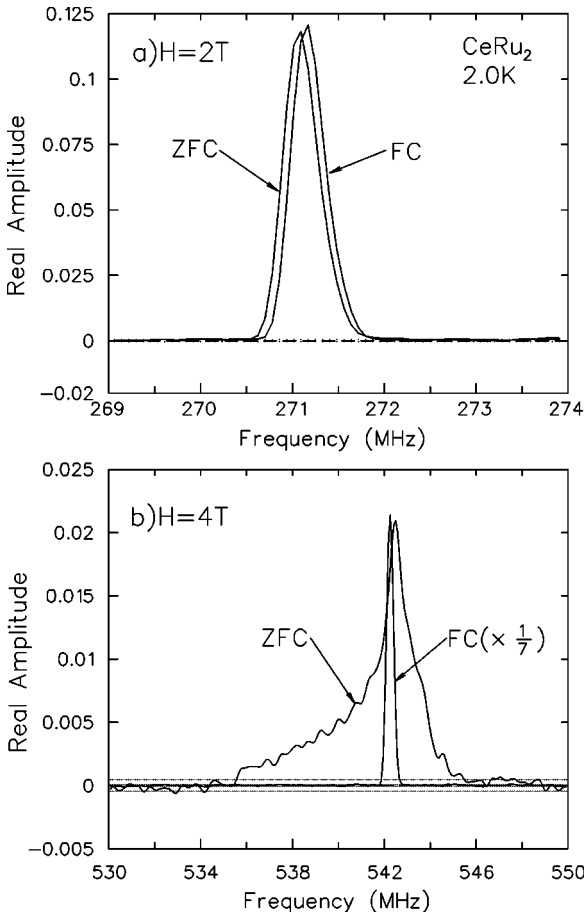

FIG. 12. FFT spectra obtained at (a) 2 T and (b) 4 T by zero field cooling (ZFC) or field cooling (FC) in $CeRu_2$ at 2.0 K.

at 4 T. Nevertheless, the line shape in Fig. 13(b) is considerably broadened due to the remaining tail around the previous field, in good contrast to Fig. 12(a) where no such broadening is observed. This indicates that the FLL exhibits residual irreversibility for a small field change such as 0.01 T, even in the presumably reversible region ($H<H^*$), probably due to the threshold for depinning. Thus, depending on the actual conditions of the field sweep, the magnetization measurement, for example, may or may not be subject to the effect of the depinning threshold.

The spectra in Fig. 13(d) have the additional feature of a low-frequency satellite that is also explained by the effect of strong pinning. Since the FLL at 4 T has a shorter lattice constant than that at 3.99 T, the fraction held at 4 T is virtually ''compressed'' from the rest. This compression must be balanced by another fraction that has ''expanded'' from the mean lattice constant for 3.99 T, yielding the low-frequency satellite peak. A similar situation is observed in Fig. 12(b) on a much larger scale, where the spectrum has a low-field tail associated with the increased field in the strongly irreversible region. Because of such a large fraction with an expanded lattice, an almost equivalent fraction exhibits compressed FLL to conserve the net magnetic induction.

V. DISCUSSION AND CONCLUSIONS

In the previous section we showed that there are two major issues that remain to be understood, i.e., (i) the strong nonlinearity in the magnetic field dependence of $\lambda(H)$, and (ii) the weak temperature dependence of $\rho_v(T)$. We must recognize that the characteristic line shape associated with $n(B)$ is less distinct in FFT spectra above 3 T and that a reasonable fit could be obtained by setting λ to the value at the lower field and allowing ξ_v to vary along the field. Nevertheless, ξ_v increases with increasing field, which is no less anomalous than the alternative case. Thus, the physical meaning of these anomalies, in any case, is clear in the sense that they are the consequence of anomalously enhanced quasiparticle excitation arising either outside (λ) or inside ($\xi_v \sim \rho_v$) the vortex cores. Since the core radius ρ_v is well reproduced by Eq. (4.5), it is reasonable to presume that the cutoff parameter obeys the same power law. Then, the observed anomaly of the linewidth is uniquely attributed to that of λ. Our primary interest is in the nonlinear field dependence of $\lambda(H)$ that is related to the possible new mixed state, and therefore, our following discussion is focused mostly on this issue.

There are three experimental findings that indicate an anomaly in the quasiparticle excitation spectrum in $CeRu_2$ at higher magnetic fields.

(1) The magnetic penetration depth $\lambda(H)$ exhibits a steep increase with increasing field for $H/H_{c2}>0.6$ (present result).

(2)The magnitude of paramagnetic moment measured by the neutron diffraction does not decrease below T_c at 3 T.[66]

(3) de Haas–van Alphen oscillation is observed deep in the mixed state (e.g., $H>0.4H_{c2}$ for the $\epsilon_{1,2,3}$ branch).[16]

It is inferred from these findings that the quasiparticle excitation is subject to anomalous enhancement in $CeRu_2$ compared with conventional type-II superconductors with *s*-wave pairing. Then, the issue is whether or not this anomalous quasiparticle excitation can be understood within the bounds of the conventional model. One such attempt based on the Ginzburg-Landau theory with quasiclassical approximation[90] shows that the quasiparticle DOS may exhibit a *field-induced* anisotropic enhancement around the equatorial directions (relative to the direction of magnetic field) on the Fermi surface.[16] However, the relevant theory is known to be accurate only near H_{c2} and therefore a more rigorous theory based on the Bogoliubov–de Gennes approach would be required for further discussion. Another possibility is to attribute the anomaly to the *intrinsic* anisotropy of the energy gap, as in the case of YNi_2B_2C,[91] although the magnitude of anisotropy in $CeRu_2$ suggested[25] by NQR is not very large ($\sim$0.15) and its origin is yet to be elucidated. We also note that λ in YNi_2B_2C exhibits a linear dependence on the magnetic field up to $H/H_{c2}\sim 0.7$ with a much steeper slope than that in $CeRu_2$, indicating that the effect of intrinsic anisotropy would be observed as an enhanced η in Eq. (4.10) [or even closer to the case of *d*-wave pairing described by Eq. (4.12)] at lower fields.[82] Thus, it would be difficult to explain the observed anomaly in $CeRu_2$ with this scenario. For the nonconventional approach, we

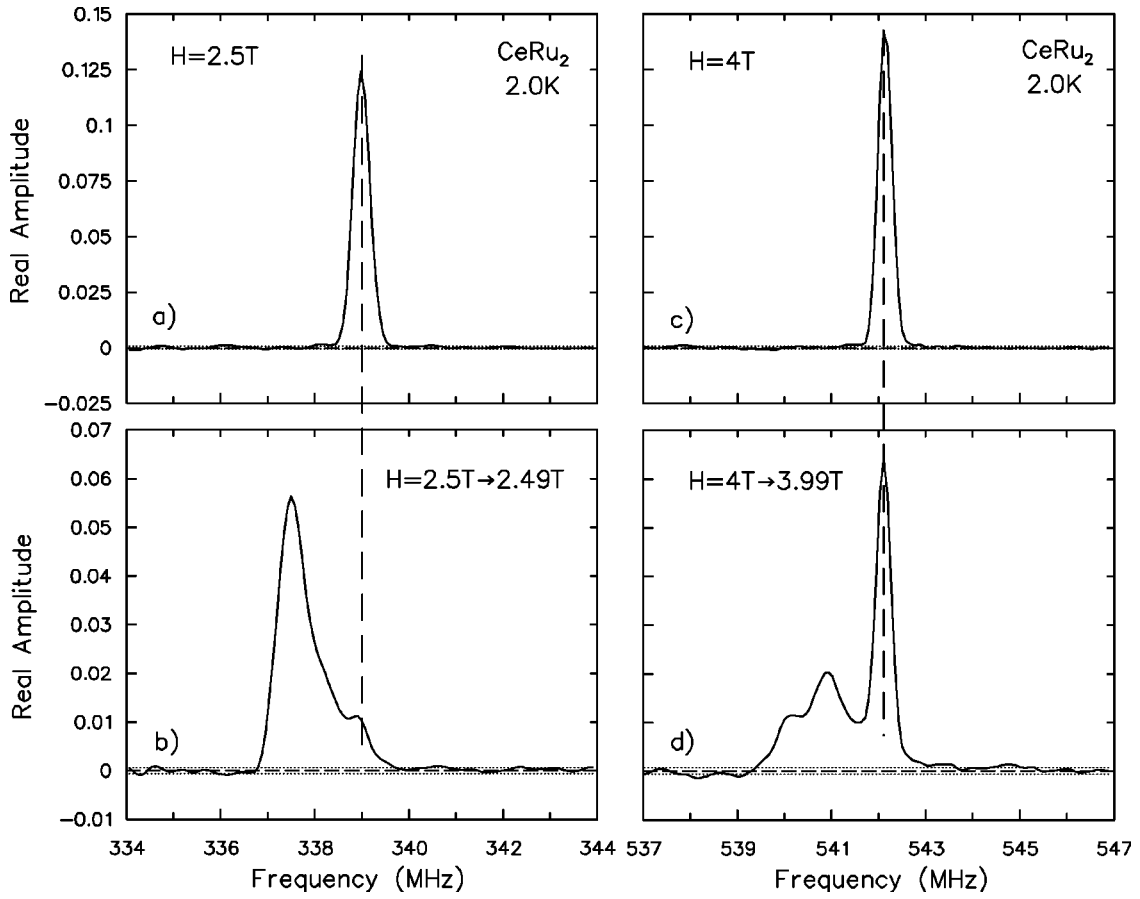

FIG. 13. FFT spectra obtained at (a) 2.5 T and (c) 4 T by field cooling (FC) in $CeRu_2$ at 2.0 K. (b) and (d) were taken just after reducing field by 0.01 T from (a) and (c), respectively.

first discuss the points raised in the arguments related to the peak effect and then examine the validity of the GFFLO model in describing the anomaly in $CeRu_2$.

The nonlinearity in $\lambda(H)$ appears over the region $H/H_{c2}=h>0.6$ where strong irreversibility sets in, as inferred from the present data in Figs. 12 and 13 as well as from the peak effect. In the usual situation, the increase of pinning leads to the enhancement of FLL disorder, which then would lead to the increase of the linewidth for the μSR spectra. Figure 7 clearly demonstrates that this is opposite to the observed tendency in the linewidth. The same is true for the effects of random local magnetic field from Ru nuclear moments and small residual field from Ce moments;[27] these local moments contribute to the *enhancement* of the muon spin relaxation rate (i.e., the broadening of the linewidth in the frequency space). Thus, we can conclude that the anomaly in $\lambda(H)$ is not an artifact of the modulated linewidth due to the spontaneous increase of the pinning force. On the other hand, the apparent correlation between the anomaly in $\lambda(H)$ and the peak effect suggests that they are two different consequences of a common origin.

In recent years, the so-called ''synchronization'' mechanism has been strongly argued to be the origin of the peak effect in $CeRu_2$. In this scenario, the shear modulus C_{66} of FLL is reduced, as inferred from Eq. (4.15), at higher fields so that the pinning becomes more efficient upon fitting the softened FLL to the random pinning centers. This is essentially the same as ''collective pinning'' as long as the pinning is due to many weak pinning centers. It should be stressed that the explanation of the peak effect due to the hypothetical FFLO (or GFFLO) state is also based on a similar mechanism, the difference being only in the origin of FLL softening. In the FFLO state, the FLL becomes soft due to the nodal planes perpendicular to the FLL. This would effectively correspond to the reduction of tilt modulus C_{44}. Moreover, even if the FFLO state is realized, the synchronization mechanism must also be in effect due to the softening of C_{66}, so that the former effect may be completely masked by that of the synchronization. Thus, it would generally be difficult in actual systems to distinguish these two mixed origins of FLL softening only by bulk measurements.

However, the microscopic natures of these two origins greatly differ. The reduction of C_{66} is not associated with the change in the superconducting order parameter and therefore the electronic structure of vortices in terms of quasiparticle excitation remains intact while the softening of FLL proceeds. The broadening of the linewidth due to the enhanced FLL distortion is the only possible consequence observed in the μSR line shape. Meanwhile, the FFLO (or GFFLO) state gives rise to the periodic nodal planes of order parameters perpendicular to vortices, leading to a drastic change in the quasiparicle excitation spectrum.

The FFLO state is expected to occur in a class of type-II superconductors that exhibit large spin susceptibilities

$$\chi_s \simeq 2\mu_B^2 D^*(\epsilon_F), \tag{5.1}$$

where the density of states at the Fermi surface $D^*(\epsilon_F) \simeq m^{*2}k_F^2/2\pi^2\hbar^2$ is enhanced by $m^*/m \simeq 2.5-3$ times the normal Pauli susceptibility, as suggested by the cyclotron mass and electronic-specific-heat coefficient. This large χ_s gives rise to a free energy $-\frac{1}{2}\chi_s h_m^2$ at the vortex cores [with $h_m \simeq B(r=0)$ being the field induced at the vortex core by the surrounding current], which may be comparable to the superconducting condensation energy at higher field. Approximating the vortex core as a cylinder of radius ρ_v, for the free energy per unit length of the vortex core, one obtains[40]

$$E_c = \pi\rho_v^2\left[\frac{H_c^2}{8\pi} - \frac{1}{2}\chi_s h_m^2\right], \tag{5.2}$$

where H_c is the thermodynamical critical field. Since $h_m \sim H$ for the relevant higher fields, the energy gain from electronic spin polarization exceeds the cost of breaking up superconducting condensation when

$$H > H_p^* \simeq H_c/2(\pi\chi_s)^{1/2} \sim \sqrt{\frac{m}{m^*}}H_p, \tag{5.3}$$

with H_p given by Eq. (4.11). We estimate $H_p^* \simeq 6.5-7$ T that turns out to be slightly larger than H_{c2}. It should be noted that E_c itself is relatively small in relevant compounds due to their short core radii. The markedly weak pinning below H^* (see Fig. 1) is explained by this small vortex-core energy below H_p^*. On the other hand, the GFFLO state presumes a new inhomogeneous mixed state at higher fields where the superconducting order parameter has periodic planar nodes, i.e.,

$$\Delta(z+L_0) = \Delta(z) \quad (=0 \quad \text{for} \quad z=0,\pm L_0, \ldots). \tag{5.4}$$

This is close to the form of the order parameter first investigated by Larkin and Ovchinnikov.[38] Detailed calculation including the effect of orbital current predicts that the order parameter near H_{c2} is approximately given by

$$\Delta(z) \simeq \Delta \sin(2\pi z/L_0) \tag{5.5}$$

with a wavelength L_0 ranging from 10ξ to 30ξ.[40] The shape of $\Delta(z)$ deviates from Eq. (5.5) toward a trapezoidal shape at lower fields, leading to a narrower region for the normal state. Since $\lambda^2 \propto 1/|\Delta|^2$, the corresponding magnetic penetration depth in the x-y plane should follow

$$\lambda^2(z) \simeq \frac{\lambda^2}{\sin^2(2\pi z/L_0)}, \tag{5.6}$$

i.e., it should show divergent increase at nodes where $\Delta(z) = 0$. Assuming that the muon probes the above distribution of $\lambda(z)$ at random (which is justified by the prediction that L_0 is of the same order of magnitude as λ), the increase of λ observed at higher fields is readily explained in the same manner as that of an average linewidth calculated from Eqs. (4.3) and (5.6),

$$\begin{aligned}\sigma_{\mathrm{FFLO}} &= \Lambda(H)\int \frac{dz/L_0}{\lambda^2(z)} \\ &= \Lambda(H)\int_{-\pi}^{\pi} \frac{\sin^2\zeta\, d\zeta}{\lambda^2} \\ &= \Lambda(H)(\sqrt{2}\lambda)^{-2},\end{aligned} \tag{5.7}$$

which is equivalent to the linewidth determined by an effective penetration depth $\bar{\lambda} \equiv \sqrt{2}\lambda$. Since the asymmetric feature of $\bar{n}(B)$ is greatly weakened due to the reduced linewidth at higher fields, the net line shape is predominantly determined by this effective linewidth σ_{FFLO}. Therefore, when the data are analyzed using the modified London model, one observes the gradual shift of field dependence from $\lambda(H)$ to $\bar{\lambda}(H) = \sqrt{2}\lambda(H)$. Thus, the presence of the GFFLO state explains the result of Fig. 8(a) qualitatively.

However, the current model of the GFFLO state has some problems that must be settled in order to quantitatively describe the observed properties in $CeRu_2$. In particular, the estimated lower boundary of the GFFLO state, H_p^*, is close to H_{c2} and thus much larger than the field above which the steep increase of λ (and hence of the quasiparticle density) was observed ($\sim 0.6H_{c2}$). This discrepancy has been one of the strong bases for maintaining the negative argument against the presence of the GFFLO state in $CeRu_2$, together with the absence of a paramagnetic effect on the Maki parameter κ_2. A similar problem has been pointed out by Tachiki *et al.*,[40] who found that the estimated effect of orbital current was too small to explain the onset of the GFFLO state at such a low field. Nevertheless, they also admitted that the estimation was based on a simple quasi-free-electron model [which is evident in Eq. (5.3), for example] and that therefore, further development of the theory is needed before the detailed electronic structure characteristic of the mixed valent compounds can be considered.

One of the less critical but important issues is the reproducibility (or lack) of hysteresis associated with the first-order phase transition. Unfortunately, this seems to be difficult to settle because the singularity (i.e., the magnitude of discontinuity in the free energy) upon the onset of the GFFLO state seems to be rather small at the phase boundary. The order parameter along the direction of vortices takes a trapezoidal form with relatively thin layers of normal states in longer periods, which leads to the small change, for example, in the effective penetration depth. This would also be the case for other bulk physical quantities such as specific heat, thermal conductivity, and magnetization. In particular, the interpretation of the magnetization process seems to have its own problem. As shown in Fig. 13, the magnetization measurements in $CeRu_2$ always bear a nonequilibrium FLL configuration depending on the step size of field modulation. This transient nature often leads to a hysteresis which is not related to phase transition.[57,58] Moreover, the magnetization measurements suffer further complication due to the coexist-

ing effect of conventional FLL softening at higher fields [see Eq. (4.15)], which makes it difficult to extract the effect associated with different origins of FLL softening. In any case, our result indicates that the anomaly in λ develops gradually for $H/H_{c2}>0.6$, suggesting that it might be difficult to observe the hysteresis associated with the phase transition.

In conclusion, we have presented microscopic evidence that the quasiparticle excitation spectrum is anomalously enhanced in $CeRu_2$ at higher fields ($H>0.6H_{c2}$), as evidenced from the strong nonlinear field dependence of $\lambda(H)$. This result is in line with the anomalous behavior of paramagnetic moments observed by neutron scattering. While the presence of this anomaly coincides with the peak effect in the magnetization process, the conventional arguments to account for the peak effect without resorting to a novel mixed state are not successful in explaining the strongly enhanced quasiparticle excitation inferred from these anomalies. On the other hand, the model of the generalized FFLO state seems to provide a qualitative account of the enhanced quasiparticle excitation at higher fields, despite the difficulty in showing a quantitative agreement with our result. In this sense, the presence of a novel mixed state in $CeRu_2$ remains yet a possibility, with the revised model of the GFFLO state being one of the candidates for such a novel state.

ACKNOWLEDGMENTS

We appreciate the hospitality of TRIUMF while this work was conducted. This work was partially supported by a Grant-in-Aid for Scientific Research on Priority Areas and a Grant-in-Aid for Scientific Research COE (10CE2004) from the Ministry of Education, Culture, Sports, Science, and Technology, Japan, and also by a grant from the CREST, JST, Japan.

*Also at CREST, Japan Science and Technology Corporation (JST), Kawaguchi, Saitama 332-0012, Japan.

†Present address: College of Science, University of Ryukyus, 1 Senbaru, Nishihara, Okinawa 903-0213, Japan.

‡Also at Advanced Science Research Center, Japan Atomic Energy Research Institute, Tokai, Ibaraki 319-1195, Japan.

[1] B. T. Mathias, H. Shul, and E. Corenzwit, Phys. Rev. Lett. **1**, 92 (1958).

[2] B. T. Mathias, H. Shul, and E. Corenzwit, Phys. Rev. Lett. **1**, 449 (1958).

[3] B. Hillenbrand and M. Wilhelm, Phys. Lett. **31A**, 448 (1971).

[4] J. W. Lynn, D. E. Moncton, L. Passell, and W. Thomlinson, Phys. Rev. B **21**, 70 (1980).

[5] J. A. Fernandez-Baca and J. W. Lynn, J. Appl. Phys. **52**, 2183 (1981).

[6] J. W. Allen, S. J. Oh, I. Lindau, M. B. Maple, J. F. Suassuna, and S. B. Hagström, Phys. Rev. B **26**, 445 (1982).

[7] D. J. Peterman, J. H. Weaver, M. Croft, and D. T. Peterson, Phys. Rev. B **27**, 808 (1983).

[8] J. C. Fuggle, F. U. Hillebrecht, Z. Zolnierek, R. Lässer, Ch. Freiburg, O. Gunnarsson, and K. Schönhammer, Phys. Rev. B **27**, 7330 (1983).

[9] J. W. Allen, S. J. Oh, M. B. Maple, and M. S. Torikachvilli, Phys. Rev. B **28**, 5347 (1983).

[10] O. Gunnarsson, K. Schönhammer, J. C. Fuggle, F. U. Hillebrecht, J. M. Esteva, R. C. Karnatak, and B. Hillebrand, Phys. Rev. B **28**, 7330 (1983).

[11] S. Yang, H. Kumigashira, T. Yokoya, A. Chainani, T. Takahashi, H. Takeya, and K. Kadowaki, Phys. Rev. B **53**, R11946 (1996).

[12] J.-S. Kang, C. G. Olson, M. Hedo, Y. Inada, E. Yamamoto, Y. Haga, Y. Onuki, S. K. Kwon, and B. I. Min, Phys. Rev. B **60**, 5348 (1999).

[13] D. Wohlleben and J. Röhler, J. Appl. Phys. **55**, 1904 (1984).

[14] A. P. Murani and R. S. Eccleston, Physica B **241-243**, 850 (1998).

[15] M. Hedo, Y. Inada, T. Ishida, E. Yamamoto, Y. Haga, Y. Onuki, M. Higuchi, and A. Hasegawa, J. Phys. Soc. Jpn. **64**, 4535 (1995).

[16] M. Hedo, Y. Inada, K. Sakurai, E. Yamamoto, Y. Haga, Y. Onuki, S. Takahashi, M. Higuchi, T. Maehira, and A. Hasegawa, Philos. Mag. B **77**, 975 (1998).

[17] A. Yanase, J. Phys. F: Met. Phys. **16**, 1501 (1986).

[18] F. López-Aguilar, S. Balle, and J. Costa-Quintana, Phys. Rev. B **38**, 163 (1988); J. Costa-Quinta, E. González-León, F. López-Aguilar, L. Puig-Puig, M. M. Sánchez-López, Physica B **206-207**, 186 (1995).

[19] M. Higuchi and A. Hasegawa, J. Phys. Soc. Jpn. **65**, 1302 (1996).

[20] A. D. Huxley, C. Paulsen, O. Laborde, J. L. Tholence, D. Sanchez, A. Junod, and R. Calemczuk, J. Phys.: Condens. Matter **5**, 7709 (1993).

[21] M. Hedo, Y. Inada, E. Yamamoto, Y. Haga, Y. Onuki, Y. Aoki, T. D. Matsuda, H. Sato, and S. Takahashi, J. Phys. Soc. Jpn. **67**, 272 (1998).

[22] K. Matsuda, Y. Kohori, and T. Kohara, J. Phys. Soc. Jpn. **64**, 2750 (1995).

[23] K. Ishida, H. Mukuda, Y. Kitaoka, K. Asayama, and Y. Onuki, Z. Naturforsch., A: Phys. Sci. **51a**, 793 (1996).

[24] H. Matsui, T. Yasuda, M. Hedo, R. Settai, Y. Onuki, E. Yamamoto, Y. Haga, and N. Toyota, J. Phys. Soc. Jpn. **67**, 3580 (1998).

[25] H. Mukuda, K. Ishida, Y. Kitaoka, and K. Asayama, J. Phys. Soc. Jpn. **67**, 2101 (1998).

[26] T. Nakama, M. Hedo, T. Maekawa, M. Higa, R. Resel, H. Sugawara, R. Settai, Y. Onuki, and K. Yagasaki, J. Phys. Soc. Jpn. **64**, 1471 (1995).

[27] A. D. Huxley, P. Dalmas de Réotier, A. Yaouanc, D. Caplan, M. Couach, P. Lejay, P. C. M. Gubbens, and A. M. Mulders, Phys. Rev. B **54**, R9666 (1996).

[28] S. B. Roy, Philos. Mag. B **65**, 1435 (1992).

[29] K. Yagasaki, M. Hedo, and T. Nakama, J. Phys. Soc. Jpn. **62**, 3825 (1993).

[30] A. B. Pippard, Philos. Mag. **19**, 217 (1969).

[31] A. M. Campbell and J. E. Evetts, Adv. Phys. **21**, 199 (1972).

[32] A. I. Larkin and Yu. N. Ovchinnikov, J. Low Temp. Phys. **34**, 409 (1979).

[33] H. Sugawara, H. Sato, T. Yamazaki, N. Kimura, R. Settai, and Y. Onuki, J. Phys. Soc. Jpn. **64**, 4849 (1995).

[34] K. Kadowaki, H. Takeya, and K. Hirata, Phys. Rev. B **54**, 462 (1996).

[35] R. Modler, P. Gegenwart, M. Lang, M. Deppe, M. Weiden, T. Lühmann, C. Geibel, F. Steglich, C. Paulsen, J. L. Tholence, N. Sato, T. Komatsubara, Y. Onuki, M. Tachiki, and S. Takahashi, Phys. Rev. Lett. **76**, 1292 (1996); F. Steglich, R. Modler, P. Gegenwart, M. Deppe, M. Weiden, M. Lang, C. Geibel, T. Lühmann, C. Paulsen, J. L. Tholence, Y. Onuki, M. Tachiki, and S. Takahashi, Physica C **263**, 498 (1996).

[36] H. Goshima, T. Suzuki, T. Fujita, R. Settai, H. Sugawara, and Y. Onuki, Physica B **223-224**, 172 (1996).

[37] P. Fulde and R. A. Ferrell, Phys. Rev. **135**, 550 (1964).

[38] A. I. Larkin and Yu. N. Ovchinnikov, Zh. Éksp. Teor. Fiz. **47**, 1136 (1964) [Sov. Phys. JETP **20**, 762 (1965)].

[39] L. W. Gruenberg and L. Gunther, Phys. Rev. Lett. **16**, 996 (1966).

[40] M. Tachiki, S. Takahashi, P. Gegenwart, M. Weiden, M. Lang, C. Geibel, F. Steglich, R. Modler, C. Paulsen, and Y. Önuki, Z. Phys. B: Condens. Matter **100**, 369 (1996); S. Takahashi, M. Tachiki, R. Modler, P. Gegenwart, M. Lang, and F. Steglich, Physica C **263**, 30 (1996).

[41] K. Goos, R. Modler, H. Schimanski, C. D. Bredl, C. Geibel, F. Steglich, A. I. Buzdin, N. Sato, and T. Komatsubara, Phys. Rev. Lett. **70**, 501 (1993).

[42] K. Tenya, M. Ikeda, T. Tayama, H. Mitamura, H. Amitsuka, T. Sakakibara, K. Maezawa, N. Kimura, R. Settai, and Y Onuki, J. Phys. Soc. Jpn. **64**, 1063 (1995).

[43] F. Thomas, B. Wand, T. Lühmann, P. Gegenwart, G. R. Stewart, F. Steglich, J. P. Brison;, A. Buzdin, L. Glemot, and J. Flouquet, J. Low Temp. Phys. **102**, 117 (1996).

[44] S. B. Roy and P. Chaddah, Phys. Rev. B **55**, 11 100 (1997).

[45] S. B. Roy and P. Chaddah, J. Phys.: Condens. Matter **9**, L625 (1997).

[46] S. B. Roy, P. Chaddah, and L. E. DeLong, Physica C **304**, 43 (1998).

[47] S. B. Roy, P. Chaddah, and S. Chaudhary, J. Phys.: Condens. Matter **10**, 4885 (1998); **10**, 8327 (1998).

[48] S. B. Roy, S. Chaudhary, P. Chaddah, and L. F. Cohen, Physica C **322**, 115 (1999).

[49] S. B. Roy and P. Chaddah, Physica B **262**, 20 (1999).

[50] S. B.Roy, P. Chaddah, and S. Chaudhary, Solid State Commun. **109**, 427 (1999).

[51] S. Chaudhary, S. B. Roy, and P. Chaddah, Solid State Commun. **111**, 263 (1999).

[52] S. Chaudhary, A. K. Rajarajan, K. J. Singh, S. B. Roy, and P. Chaddah, Solid State Commun. **114**, 5 (2000).

[53] S. Chaudhary, S. B. Roy, and P. Chaddah, Physica B **280**, 229 (2000).

[54] G. Ravikumar, T. V. C. Rao, P. K. Mishra, V. C. Sahni, S. Saha, S. S. Banerjee, N. G. Patil, A. K. Grover, S. Ramakrishnan, S. Battacharya, E. Yamamoto, Y. Haga, M. Hedo, Y. Inada, and Y. Onuki, Physica C **276**, 9 (1997).

[55] N. R. Dilley and M. B. Maple, Physica C **278**, 207 (1997).

[56] D. Groten, S. Ramakrishnan, G. J. Nieuwenhuys, and J. A. Mydosh, Physica C **306**, 271 (1998).

[57] G. Ravikumar, V. C. Sahni, P. K. Mishra, T. V. C. Rao, S. S. Banerjee, A. K. Grover, S. Ramakrishnan, S. Battacharya, M. J. Higgins, E. Yamamoto, Y. Haga, M. Hedo, Y. Inada, and Y. Onuki, Phys. Rev. B **57**, R11 069 (1998).

[58] S. S. Banerjee, N. G. Patil, S. Saha, S. Ramakrishnan, A. K. Grover, S. Battacharya, G. Ravikumar, P. K. Mishra, T. V. C. Rao, V. C. Sahni, M. J. Higgins, E. Yamamoto, Y. Haga, M. Hedo, Y. Inada, and Y. Onuki, Phys. Rev. B **58**, 995 (1998).

[59] K. Tenya, S. Yasunami, T. Tayama, H. Amitsuka, T. Sakakibara, M. Hedo, Y. Inada, E. Yamamoto, Y. Haga, and Y. Onuki, J. Phys. Soc. Jpn. **68**, 224 (1999).

[60] N. R. Dilley J. Herrmann, S. H. Han, M. B. Maple, S. Spagna, J. Diederichs, and R. E. Sager, Physica C **265**, 150 (1996).

[61] H. Sato, Y. Kobayashi, H. Sugawara, Y. Aoki, R. Settai, and Y. Onuki, J. Phys. Soc. Jpn. **65**, 153 (1996); H. Sato, Y. Aoki, Y. Kobayashi, H. R. Sato, T. Nishigaki, H. Sugawara, M. Hedo, Y. Inada, and Y Onuki, Phys. Rev. B **230-232**, 402 (1997).

[62] N. R. Dilley, J. Herrmann, S. H. Han, and M. B. Maple, Phys. Rev. B **56**, 2379 (1997).

[63] M. Hedo, Y. Kobayashi, Y. Inada, E. Yamamoto, Y. Haga, J. Suzuki, N. Metoki, Y. Onuki, H. Sugawara, H. Sato, K. Tenya, T. Tayama, H. Amitsuka, and T. Sakakibara, J. Phys. Soc. Jpn. **67**, 3561 (1998).

[64] S. Matsuo, S. Higashitani, Y. Nagato, and K. Nagai, J. Phys. Soc. Jpn. **67**, 280 (1998).

[65] D. Saint-James *et al.*, in *Type II Superconductivity* (Pergamon Press, Oxford, 1969), Chaps. 5, 6.

[66] A. Huxley, J. X. Boucherle, M. Bonnet, F. Bourdarot, I. Schustler, D. Caplan, E. Lelievre, N. Bernhoeft, P. Lejay, and B. Gillon, J. Phys.: Condens. Matter **9**, 4185 (1997).

[67] C. G. Shull and F. A. Wedgewood, Phys. Rev. Lett. **16**, 513 (1966).

[68] A. Yamashita, K. Ishii, T. Yokoo, J. Akimitsu, M. Hedo, Y. Inada, Y. Onuki, E. Yamamoto, Y. Haga, and R. Kadono, Phys. Rev. Lett. **79**, 3771 (1997).

[69] R. H. Norton and R. Beer, J. Opt. Sci. Soc. Am. **66**, 259 (1976); **67**, 419 (1976).

[70] E. H. Brandt, J. Low Temp. Phys. **26**, 709 (1977); **73**, 355 (1988); Phys. Rev. B **37**, 2349 (1988).

[71] W. G. Clark, F. Lefloch, and W. H. Wong, Phys. Rev. B **52**, 7488 (1995).

[72] A. Huxley, R. Cubitt, D. McPaul, E. Forgan, M. Nutley, H. Mook, M. Yethiraj, P. Lejay, D. Caplan, and J. M. Pénisson, Physica B **223&224**, 169 (1996).

[73] J. Suzuki, N. Metoki, Y. Haga, E. Yamamoto, H. Kadowaki, K. Kakurai, M. Hedo, and Y. Onuki, Physica B **241-243**, 871 (1998).

[74] H. Sakata, N. Nishida, M. Hedo, K. Sakurai, Y. Inada, Y. Onuki, E. Yamamoto, and Y. Haga, Physica B **223&224**, 169 (1996).

[75] A. Yaouanc, P. Dalmas de Réotier, and E. H. Brandt, Phys. Rev. B **55**, 11 107 (1997).

[76] I. G. de Oliveira and A. M. Thompson, Phys. Rev. B **57**, 7477 (1998).

[77] T. M. Riseman, J. H. Brewer, K. H. Chow, W. N. Hardy, R. F. Kiefl, S. R. Kreitzman, R. Liang, W. A. MacFarlane, P. Mendels, G. D. Morris, J. Rammer, J. W. Schneider, C. Niedermayer, and S. L. Lee, Phys. Rev. B **52**, 10 569 (1995).

[78] M. Ichioka, A. Hasegawa, and K. Machida, Phys. Rev. B **59**, 184 (1999).

[79] G. E. Volovik, Pis'ma Zh. Éksp. Teor. Fiz. **58**, 457 (1993) [JETP Lett. **58**, 469 (1993)].

[80] J. E. Sonier, J. H. Brewer, R. F. Kiefl, D. A. Bonn, S. R. Dunsiger, W. N. Hardy, R. Liang, W. A. MacFarlane, R. I. Miller, and T. M. Riseman, Phys. Rev. Lett. **79**, 2875 (1997).

[81] J. E. Sonier, R. F. Kiefl, J. H. Brewer, J. Chakhalian, S. R. Dun-

siger, W. A. MacFarlane, R. I. Miller, and A. Wong, Phys. Rev. Lett. **79**, 1742 (1997).
[82] K. Ohishi, K. Kakuta, J. Akimitsu, W. Higemoto, R. Kadono, R. I. Miller, A. Price, R. F. Kiefl, J. E. Sonier, M. Nohara, H. Suzuki, and H. Takagi, Physica B **289-290**, 377 (2000).
[83] W. Pesch and L. Kramer, J. Low Temp. Phys. **15**, 367 (1974).
[84] L. Kramer and W. Pesch, Z. Phys. **269**, 59 (1974).
[85] C. Caroli, P. G. de Gennes, and J. Matricon, Phys. Lett. **9**, 307 (1964).
[86] F. Gygi and M. Schlüter, Phys. Rev. B **43**, 7609 (1991).
[87] N. Hayashi, T. Isoshima, M. Ichioka, and K. Machida, Phys. Rev. Lett. **80**, 2921 (1998).
[88] R. I. Miller, R. F. Kiefl, J. H. Brewer, J. Chakhalian, S. Dunsiger, G. D. Morris, J. E. Sonier, and W. A. MacFarlane, Phys. Rev. Lett. **85**, 1540 (2000).
[89] B. Mühlschlegel, Z. Phys. **155**, 313 (1959).
[90] K. Maki, Phys. Rev. B **44**, 2861 (1991).
[91] T. Yokoya, T. Kiss, T. Watanabe, S. Shin, M. Nohara, H. Takagi, and T. Oguchi, Phys. Rev. Lett. **85**, 4952 (2000).